Systems & Control Transactions

Research Article - Peer Reviewed Conference Proceeding
ESCAPE 35 - European Symposium on Computer Aided Process Engineering
Ghent, Belgium. 6-9 July 2025
Jan F.M. Van Impe, Grégoire Léonard, Satyajeet S. Bhonsale,
Monika E. Polańska, Filip Logist (Eds.)

PSE PRESS

Optimisation of a Haber-Bosch Synthesis Loop for PtA

Joachim W. Rosbo[a], Anker D. Jensen[a], John B. Jørgensen[b], Sigurd Skogestad[c] and Jakob. K. Huusom[a]*

[a] Technical University of Denmark, Department of Chemical Engineering, Kgs. Lyngby, Denmark
[b] Technical University of Denmark, Applied Mathematics and Computer Science, Kgs. Lyngby, Denmark
[c] Norwegian University of Science and Technology, Department of Chemical Engineering, Trondheim, Norway
* Corresponding Author: jhk@kt.dtu.dk.

ABSTRACT

This work presents a plantwide model of a Haber-Bosch ammonia synthesis loop (HB-loop) in a PtA plant, consisting of heat exchangers, compressors, steam turbines, flash separators and catalytic reactor beds. The total electrical power utility of the HB-loop is a combination of compressor power, refrigeration power, and steam turbine power. We optimise the HB-loop operating parameters, subject to constraints for maximum reactor temperatures, compressor choke and stall, minimum steam temperature, and maximum loop pressure. The loop features six degrees of freedom (DOFs) for the optimisation: three reactor temperatures, reactor N_2/H_2-ratio, separator temperature, and loop pressure. The optimisation minimises the total loop power utility for a given hydrogen make-up feed flow, with the PtA load varied by ranging the hydrogen make-up feed flow from 10 % to 120 % of the nominal. Across this load range, different constraints become active, with the compressor surge limit being particularly critical at low loads, significantly increasing HB-loop power consumption. To address this, we investigate configurations with two, three, and four compressor trains operating in parallel. Reductions in total power of 55%, 74%, and 84% are achieved at reduced plant loads, with two, three, and four parallel trains, respectively. In terms of total compressor capital and operating cost, we demonstrated savings of 8.06%, 8.29%, and 7.11% in total cost after ten years of operation with two, three, and four parallel compressor trains compared to a single train configuration.

Keywords: Power-to-Ammonia, Synthesis loop model, Optimisation, Parallel compressors.

1 INTRODUCTION

Power-to-X (PtX) is one of the most promising solutions for long-term storage of renewable energy such as wind and solar power [1]. Among the various PtX technologies, Power-to-Ammonia (PtA) receives significant attention due to its ability to store and recover energy without carbon dioxide emissions. PtA employs the traditional Haber-Bosch synthesis loop but with hydrogen produced via electrolysis rather than steam-methane reforming and nitrogen from air separation. The hydrogen production consumes around 90 % of the total plant electricity and hence highly depends on the available renewable energy. Due to the intermittent nature of renewable power sources, the synthesis loop is required to operate across a broad operating envelope from 10 % to 120 % of the nominal synthesis feed flow [2]. In [3], we developed dynamic models for three general ammonia reactor types: adiabatic quench-cooled (AQCR), adiabatic indirect-cooled (AICR), and internal direct-cooled reactors (IDCR). These reactors were optimised across a wide range of feed flow rates and evaluated for flexibility and robustness in a PtA plant, with the AICR and IDCR identified as the most suitable options.

In this work, we expand the scope by introducing a model for the entire HB synthesis loop, including an AICR reactor. The study focuses on optimising the HB-loop across the operating range from 10 % to 120 % of the nominal hydrogen make-up feed flow. We evaluate different loop designs with multiple parallel compressors to identify the most economical configuration.

2 SYNTHESIS LOOP MODEL AND OPTIMISATION

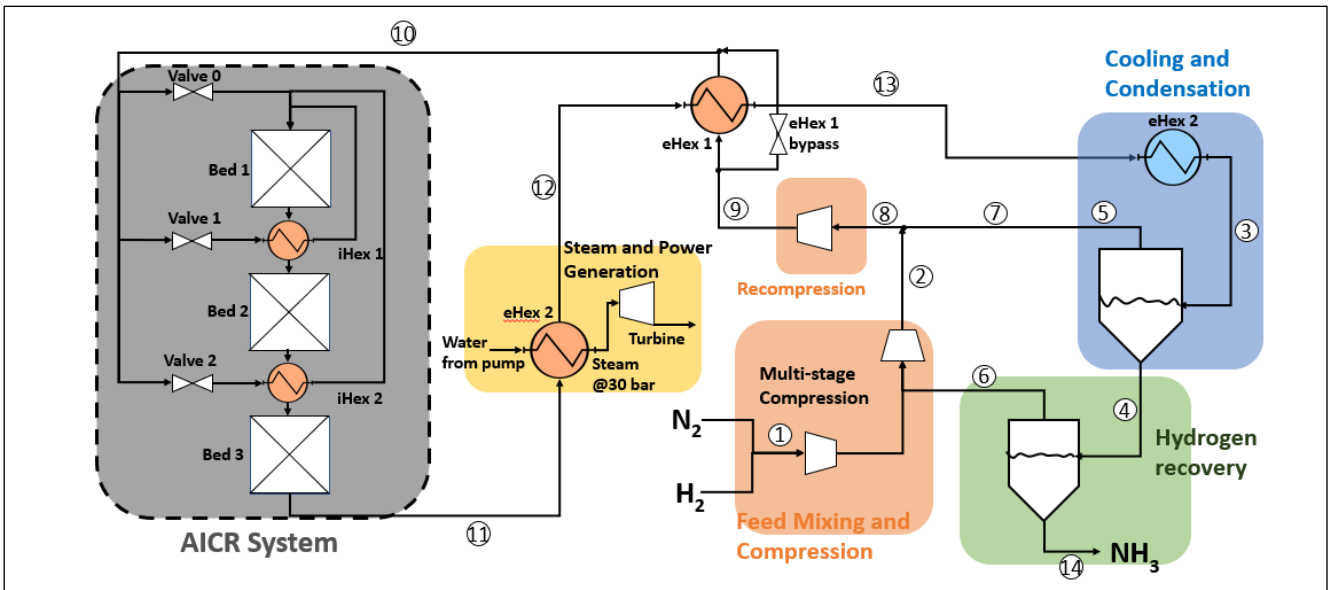

Figure 1: Schematic illustration of the Haber Bosch synthesis loop with an adiabatic indirect cooled reactor (AICR). Streams connecting the operating units are numbered as indicated in the diagram.

Figure 1 shows the Haber-Bosch ammonia synthesis loop. The make-up gas of hydrogen and nitrogen is compressed to the high synthesis loop pressure (>80 bar) and preheated before entering the reactor. The nitrogen feed, produced via air separation, contains 0.1% argon, significantly lower than the 1.2% found in conventional ammonia plants, where the nitrogen is supplied directly from combustion air. This eliminates the need for a purge stream in the synthesis loop as the solubility in the liquid ammonia product stream balances the argon build-up.

2.1 Reactor and heat exchanger model

The AICR consists of a combination of catalytic fixed beds and counter-current heat exchanges. The catalytic beds are assumed to be adiabatic and modelled in one dimension along the axial direction. Furthermore, we assume no transport limitations within the catalytic particles, which implies isothermal catalytic particle phase and gas phase. The reactor model is extensively described in [3]. The pressure drop across the catalytic bed is determined using Ergun's equation,

$$\frac{\mathrm{d}P}{\mathrm{d}l} = \frac{180\mu^g}{d_p^2}\frac{(1-\epsilon)^2}{\epsilon^3}v_s + \frac{1.75\rho^g}{d_p}\frac{(1-\epsilon)}{\epsilon^3}v_s^2, \qquad (1)$$

in which P is the pressure, μ^g is the gas viscosity, ρ^g is the gas density, d_p is the hydraulic diameter of the catalyst particles and v_s is the superficial gas velocity.

2.2 Compressor model

Centrifugal compressors are employed in the ammonia synthesis loop to compress the make-up feed gas and re-compress the recycle stream. The compressors are modelled based on isentropic compression from inlet pressure, P_1, to outlet pressure P_2,

$$S(T_1, P_1, F_{comp.}) = S(T_s, P_2, F_{comp.}), \qquad (2a)$$

$$W_{s,\ comp.} = H(P_{out}, T_s, N) - H(P_{in}, T_{in}, N), \qquad (2b)$$

with $W_{s,\ comp.}$ being the work of the isentropic compression. The real outlet temperature, T_2, and work, $W_{comp.}$, are found by solving,

$$\eta_s W_{comp.} = W_{s,\ comp.}, \qquad (2c)$$

$$W_{comp.} = H(T_2, P_2, F_{comp.}) - H(T_1, P_1, F_{comp.}), \qquad (2d)$$

where η_s is the isentropic efficiency. The compressor efficiency is assumed to follow a polynomial expression as a function of the corrected flow, $F_{cor.}$,

$$\eta_s(F_{cor.}) = -0.44\left(\frac{F_{cor.}}{F_{n,\ comp.}}\right)^2 + 0.85\left(\frac{F_{cor.}}{F_{n,\ comp.}}\right) + 0.35, \qquad (2e)$$

where $F_{n,\ comp.}$ is the nominal compressor flow. The corrected flow is given by, $F_{cor} = F_{comp.}\frac{P_1}{P_{1n}}$, with P_1 being the compressor inlet pressure and P_{1n} the inlet pressure at the design point. The coefficients of the polynomial ($a = -0.44, b = 0.85, c = 0.35$) are determined from a qualitative fit of a compressor map generated with `Concept NREC`® design software for the relevant [N_2,H_2,Ar,NH_3] gas mixture [4]. Furthermore, to prevent compressor surge and choke, the operating range of the compressors is restricted between 65 % and 130 % of the nominal compressor flow. Below 65 % corrected compressor flow, anti-surge recycle control is activated. The feed gas compression is performed using multistage compressors with a maximum compression ratio of 3.5 per stage.

2.3 Separator model

Due to the large difference in boiling points between ammonia and the synthesis gas, the product separation

Table 1: Optimal operating parameters and power distribution at nominal load.

Optimal parameters		Power distribution	
Bed inlet temperatures [K]	[724, 704, 694]	Feed compression	5.50 MW
Reactor inlet pressure	206.8 bar	Recycle compression	0.18 MW
Separator temperature	25 °C	Steam generator	3.60 MW
Reactor H_2/N_2-ratio	2.71	Refrigeration power	0 MW
		HB-loop power	**2.11 MW**

is achieved via a flash tank. The material balance over the flash tank is,

$$0 = F^{l}_{sep.} + F^{g}_{sep.} - F_{f,\ sep.}\,, \tag{3a}$$

where $F_{f,\ sep.}$ is the separator inlet flow, and $F^{l}_{sep.}$ and $F^{g}_{sep.}$ are respectively the liquid and gas flow exiting the separator. At vapour-liquid equilibrium the component chemical potentials of the phases are identical,

$$0 = \mu^{g}_{i}\left(T_{sep.}, P_{sep.}, x^{g}\right) - \mu^{l}_{i}\left(T_{sep.}, P_{sep.}, \mathrm{x}^{l}\right), \tag{3}$$

in which the chemical potential, μ_i, of component i is a function of the separator temperature, T_{sep}, pressure, P_{sep}, and composition, x_{sep}. The chemical potential of the gas and liquid mixtures are calculated with the thermodynamic tool `Thermolib` [5].

2.4 Cooling and Refrigeration

Cooling is performed before the separator and between stages for make-up feed compression. We assume cooling water is available at 15 °C and the heat exchangers are designed based on a 10 °C minimum temperature approach. Therefore, cooling below 25 °C requires a refrigeration cycle. Assuming a coefficient of performance of three ($COP = 3$), typical for refrigeration around 0 °C [6], the refrigeration power for cooling before the flash tank is,

$$W_{refrigiation} = \frac{\left(\dot{H}(25.0\ ^{\circ}\mathrm{C}, P_{sep.}, F_{sep.}) - \dot{H}(T_{sep.}, P_{sep.}, F_{sep.})\right)}{COP} \tag{4}$$

in which $\dot{H}$ is the enthalpy flow of the stream at the temperature, T, pressure, P, and flow F. The enthalpy flows in Eq. 4 are for two-phase flows.

2.5 Rankine cycle

The hot outlet stream from the reactor is around 750-820 K. This temperature facilitates the generation of superheated steam at 30 bar ($T^{@30\mathrm{bar}}_{sat} = 507.0\ ^{\circ}\mathrm{C}$), driving a turbine in a Rankine cycle. We assume a heat-to-electric power efficiency of, $\eta_{rankine} = 40\ \%$, representing a high-efficiency cycle with superheated steam [6]. Thus, the generated electrical power is given by,

$$W_{rankine} = \eta_{rankine}\begin{pmatrix}\dot{H}(T^{out}_{reac.}, P^{out}_{reac.}, F^{out}_{reac.}) \\ -\dot{H}(T_{S12}, P^{out}_{reac.}, F^{out}_{reac.})\end{pmatrix} \tag{5}$$

where $\dot{H}$ is the enthalpy flow of the stream at the temperature, T, pressure, P, and flow, F. T_{S12} is the temperature of stream 12 (see Figure 1) given by $T_{S12} = T_{S10} + 10\ ^{\circ}\mathrm{C}$, where T_{S10} is reactor feed temperature. The addition of $10\ ^{\circ}\mathrm{C}$ ensures sufficient temperature driving force in the pre-reactor external heat exchanger (Figure 1: eHex 1).

2.6 Optimisation problem

The electrical power consumption of the Harber-Bosch process consists of compressor and refrigeration power, while the steam turbine generates electricity. The total external electrical utility of the HB-loop, W_{HB}, is,

$$W_{HB} = W^{feed}_{comp} + W^{recycle}_{comp} + W_{refrigiation} - W_{rankine}. \tag{6}$$

We assume cooling water is a negligible operational cost. Hence, the total electrical power utility, W_{HB}, represents the cost function for the synthesis loop. As no purge stream figures in the PtA synthesis loop (see Figure 1), all hydrogen and nitrogen leave the synthesis loop by conversion to ammonia. This entails that hydrogen and nitrogen are fed at the stoichiometric ratio. Thus, for a given hydrogen make-up feed flow, minimising W_{HB} represent the optimal solution. The optimisation involves six degrees of freedom (DOF): three reactor temperatures, N_2/H_2-ratio, separator temperature, and loop pressure. We define the DOFs in a vector, ν,

$$\nu = \left[T^{in,1}_{reac.},\ T^{in,2}_{reac.},\ T^{in,3}_{reac.}, P^{in}_{reac.}, T_{sep.}, S_{\mathrm{H_2/N_2}}\right] \tag{7}$$

The optimal solution is found minimising the objective function across the six DOFs,

$$\min_{\nu} \quad W_{HB}, \tag{8a}$$

$$\text{s.t.} \quad f\left(x, y, F_{S1,\mathrm{H_2}}\right) = 0,\ g(x, y) = 0, \tag{8b}$$

$$0.65 \leq \frac{F_{cor.}}{F_{n,\ comp.}} \leq 1.3 \tag{8c}$$

where Eq. 8b represents the steady-state solution for a given hydrogen make-up flow, $F_{S1,\mathrm{H_2}}$, with f and g denoting the rate function and the algebraic equations as described in [3]. The optimisation problem is solved using the Matlab minimisation function `fmincon`. We define the specific HB-power cost for producing ammonia as,

$$E_{\mathrm{NH_3}} = \frac{W_{HB}}{\dot{m}_{\mathrm{NH_3}}}, \tag{9}$$

Where $\dot{m}_{\mathrm{NH_3}}$ is the mass flow of produced ammonia from the separator.

3 RESULTS

3.1 Optimisation at nominal load

The nominal load of the HB-loop is defined relative to a hydrogen make-up flow of 1.98 ton/h, corresponding to the 100 MW PtA plant presented in [7]. Table 1 summarises the optimal operating parameters and the corresponding power distribution when solving the optimisation in Eq. 8 at nominal load. The feed compression consumes most of the electrical utility with 5.50 MW, while the recycle compression only constitutes 0.18 MW. The optimal separator temperature of 25 °C is at the lower bound for water cooling, avoiding refrigeration power. A relatively big fraction of the electrical utility for compression is regained through the Rankine cycle delivering 3.6 MW. This sums to a total of 2.11 MW of external electrical utility required to power the HB-loop.

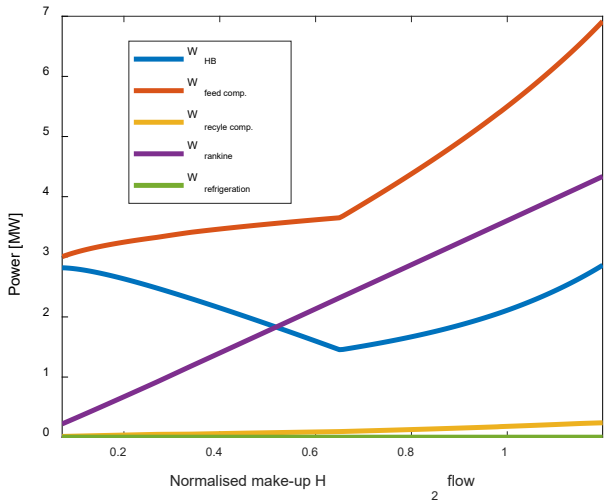

Figure 2. Distribution of power in the HB-loop across the operating envelope.

3.1 Optimisation across the operating window

We define the hydrogen load, HL, as the normalised make-up feed flow relative to the nominal flow,

$$HL = \frac{F_{S1,\mathrm{H_2}}}{F_{S1n,\mathrm{H_2}}}, \tag{10}$$

The optimisation problem in Eq. 8 is solved across the hydrogen load range from 10 % to 120 % of nominal flow. Figure 2 shows the optimal solution for the power utilities of the operating units across the operating window. The feed compressor power naturally decreases with the hydrogen load as less make-up feed gas is supplied. However, at 65 % of nominal hydrogen feed, the reduction in compressor power with hydrogen load is significantly restricted. This can be explained from Figure 3, showing the normalised corrected make-up feed and recycle flow along with the compressor surge limit across the operating envelope. The corrected feed flow intersects the surge line corresponding with the discontinuity in the feed compressor power in Figure 2. Reaching the surge line initiates the anti-surge recycling, limiting the decrease in compressor power. Figure 3 reveals that the recycle compressor reaches the surge line at a significantly lower load than the feed flow; however, its relatively smaller contribution to the total compressor power (see Figure 2) makes this effect negligible.

From Figure 2 we observe that the total HB-power, somewhat counterintuitively, increases with decreasing load when compressor anti-surge recycle is activated. This occurs because the power generated by the steam turbine decreases linearly with the hydrogen load, while the compressor power experiences only a slight reduction. Figure 4 illustrates that this dramatically impacts the specific ammonia production cost shown on the left y-axis. At reduced loads, the specific ammonia cost is up to twenty times higher relative to the nominal load. Additionally, Figure 4 displays the optimal reactor pressure across the operating envelope on the right y-axis. The optimal pressure decreases at reduced loads, explaining the slight decrease in feed compressor power seen in Figure 2 after reaching the surge limit.

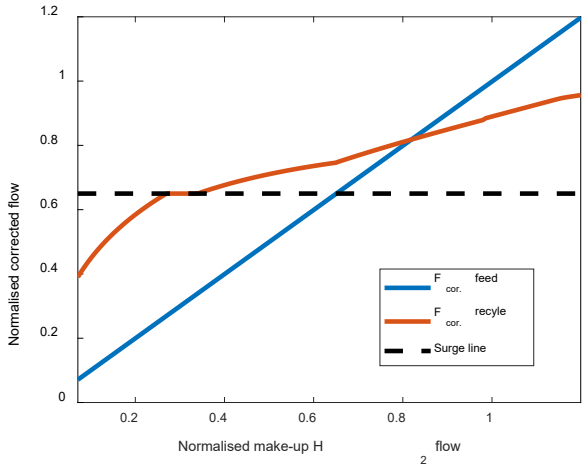

Figure 3. Normalised corrected flow for the feed and recycle compressors across the operating envelope.

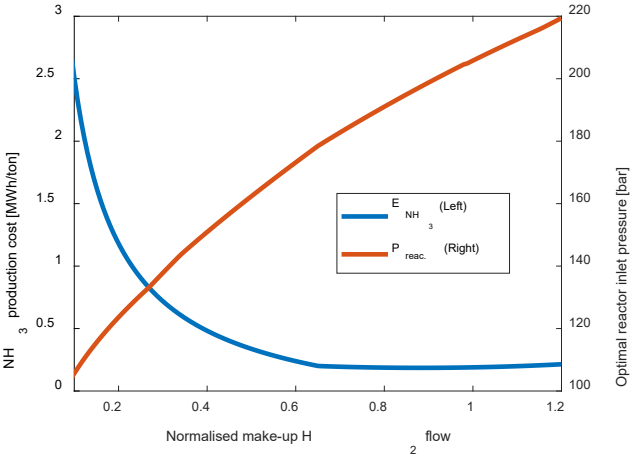

Figure 4. Left y-axis: Specific ammonia production cost.

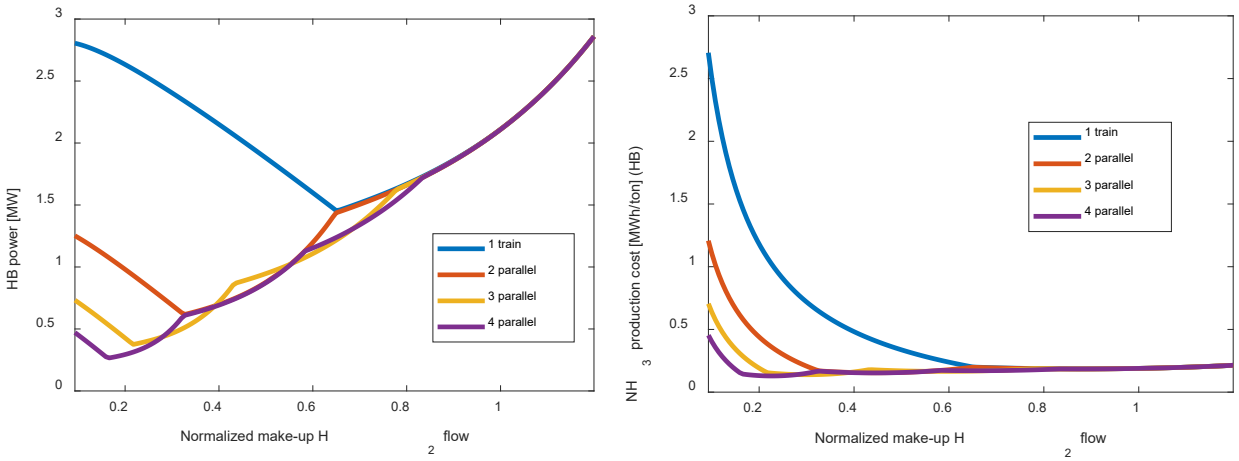

Figure 4: a) HB-power requirement and b) Specific ammonia production cost across the operating envelope with one, two, three and four parallel compressor trains.

Right y-axis: Optimal reactor pressure across the operating window.

3.1 Compressors in parallel

Figure 4 illustrates the drastic increase in ammonia production cost at low loads, caused by compressor anti-surge recycling. To reduce this loss, we investigate operating with multiple compressor trains in parallel. Parallel compressor trains extend the combined operational range of the compressors as one train can be stopped when the surge limit is reached. Additionally, multiple parallel compressors can facilitate higher compressor efficiency as the compressor flow can be distributed closer to the optimal operating flow. We solve the optimisation problem in Eq. 8 across the operating window with two, three, and four parallel compressor trains. Figure 5a displays the optimal HB-loop power for different compressor configurations, showcasing a significant reduction in HB-power by operating with multiple parallel compressor trains. At around 80 % hydrogen feed load, the configurations with 3 and 4 parallel compressor trains reduce the HB-power due to improved compressor efficiency achieved by pausing one compressor. However, the substantial reduction in HB-power occurs below the compressor surge limit, as the anti-surge recycling is shifted to 32.5 %, 21.7 % and 16.3 % of nominal hydrogen load for two, three and four parallel compressor trains, respectively.

Figure 5b shows the specific ammonia production cost across the operating envelope. Clearly, multiple parallel compressors significantly decrease production costs. At 10 % load, the ammonia production cost is reduced by 55 %, 74 % and 84 % for two, three and four parallel compressor trains, respectively.

5 ECONOMIC COMPARISON

Figures 4a and 4b illustrate that operating with multiple parallel compressor trains significantly reduces the HB-loop power during part-load operation. However, to evaluate the economic benefits, it is essential to consider the distribution of operating hours across the hydrogen loads. This is an extensive optimisation problem depending on factors such as the local wind and solar power distribution, the relative size of renewable power to the electrolyser and synthesis loop capacity, hydrogen storage size and electricity price. Performing this optimisation is not the scope of this paper, but was assessed by [2] and [8] . They concluded that wind and solar-powered PtA plants optimally operate mainly at minimum load, during periods of limited renewable power, or nominal load and above, during periods of surplus renewable energy. Complete reactor shutdown should be avoided as start-up times are extensive and frequent shutdowns damage the reactor catalyst [2,8]. Based on this, we assume an HB-loop capacity factor of 70 % with the hydrogen load distribution in Figure 5. The mean power consumption of the HB-loop is found from the probability density function, p, via,

$$\overline{W_{HB}} = \int_{0.1}^{1.2} W_{HB}(HL)p(HL)\,\mathrm{d}HL \tag{11}$$

Note p is a piecewise function from the distribution in Figure 5. Table 2 summarises the mean HB-loop power for the four parallel compressor configurations. Approximately 25 % reduction in mean HB-power is achieved by operating with two parallel compressors, while further power savings are less significant for three and four parallel compressors.

Table 2: Mean HB-power with one, two, three or four compressor trains in parallel.

Par. compressors	**1**	**2**	**3**	**4**
Mean HB-power [MW]	2.14	1.60	1.45	1.37

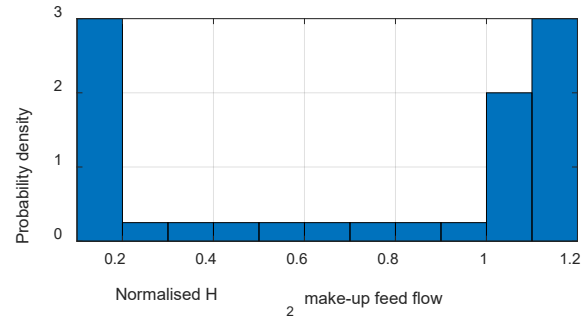

Figure 5. Probability density distribution of the synthesis loop load.

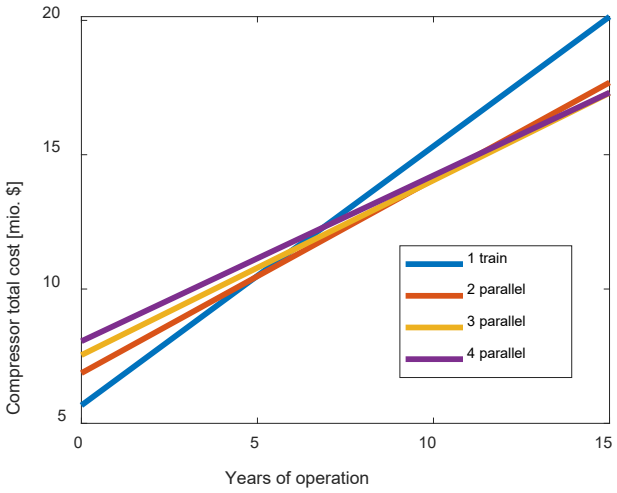

Figure 6. Total compressor cost (CAPEX + OPEX) for 15 years of operation with one, two, three or four compressor trains in parallel.

The compressor capital costs are assessed using the bare module cost (BMC) method described in [9]. Electricity is the only operational cost differentiating the parallel compressor configurations. We assume a relatively conservative electricity price of 0.045 $/kWh. Figure 7 displays the compressor systems' total cost (CAPEX + OPEX) as a function of years of operation. Naturally, the initial capital cost increases with the number of parallel compressors. However, the reduced electrical utility cost relatively quickly outweighs the additional capital costs. After ten years, operating with two, three, and four parallel compressor trains saves 8.06%, 8.29% and 7.11% of total costs, compared to a single train configuration. Additionally, from the redundancy principle, the reliability of the synthesis loop is significantly enhanced with more parallel compressors. Specifically, with three parallel trains, near full-load operation can be maintained using the remaining two compressor trains if one is out of function. Therefore, considering economic and reliability factors, we recommend the configurations with two or three parallel compressors for operation in a PtA plant.

5 CONCLUSION

In this work, we have introduced a static model of an ammonia synthesis loop to evaluate the total synthesis loop power. The power function was minimised to identify the optimal operating parameters for reactor bed inlet temperatures, reactor inlet pressure, separator temperature and reactor N_2/H_2-ratio. The optimisation was performed across the operating window from 10 % to 120% of nominal make-up feed hydrogen flow. This demonstrated that the compressor anti-surge limit strongly impacted the synthesis loop power at reduced loads. The surge boundary constrained the reduction in compressor power, resulting in an increase in total HB-loop power at low loads. To mitigate losses from anti-surge recycling, we evaluated configurations with multiple compressors operating in parallel. Optimisation results showed substantial reductions in HB-loop power at reduced loads: 55%, 74%, and 84% for two, three, and four compressor trains, respectively. This corresponded to total cost savings of 8.06%, 8.29% and 7.11%, respectively, compared to a single train configuration. Additionally, considering the enhanced reliability of configurations with parallel compressors, we recommended the configurations with two or three parallel compressor trains.

REFERENCES

1. S. Miehling, S. Fendt, and H. Spliethoff, “Optimal integration of Power-to-X plants in a future European energy system and the resulting dynamic requirements,” Energy Convers Manag, vol. 251, 2021.
2. J. Armijo and C. Philibert, “Flexible production of green hydrogen and ammonia from variable solar and wind energy: Case study of Chile and Argentina,” Int J Hydrogen Energy, vol. 45, 2020.
3. J. W. Rosbo, A. D. Jensen, J. B. Jørgensen, and J. K. Huusom, “Comparison, operation and cooling design of three general reactor types for Power-to-Ammonia processes,” Chemical Engineering Journal, vol. 496, p. 153660, 2024.
4. Concepts NREC. https://www.conceptsnrec.com/design-software-solutions
5. T. K. S. Ritschel, J. Gaspar, A. Capolei, and J. B. Jørgensen, “An open-source thermodynamic software library ”. DTU Compute-Technical Report-

2016 No. 12, 2016.
6. R. T. Balmer, “Modern Engineering Thermodymacis”. Boston: Academic Press, 2011.
7. J. W. Rosbo, T. K. S. Ritschel, S. Hørsholt, J. K. Huusom, and J. B. Jørgensen, “Flexible operation, optimisation and stabilising control of a quench cooled ammonia reactor for power-to-ammonia,” Comput Chem Eng, vol. 176, p. 108316, 2023.
8. S. Schulte Beerbühl, M. Fröhling, and F. Schultmann, “Combined scheduling and capacity planning of electricity-based ammonia production to integrate renewable energies,” Eur J Oper Res, vol. 241, pp. 851–862, 2015.
9. K. M. Guthrie, “Process plant estimating evaluation and control”, Craftsman Book Co. (U.S.A.), 1974.